

Published in final edited form as:

*Exp Cell Res.* 2014 August 1; 326(1): 78–89. doi:10.1016/j.yexcr.2014.05.018.

## Heat Shock Protein 90 $\beta$ Stabilizes Focal Adhesion Kinase and Enhances Cell Migration and Invasion in Breast Cancer Cells

Xiangyang Xiong<sup>1,2,3</sup>, Yao Wang<sup>1</sup>, Chengmei Liu<sup>3</sup>, Quqin Lu<sup>4</sup>, Tao Liu<sup>1</sup>, Guoan Chen<sup>5</sup>, Hai Rao<sup>6</sup>, and Shiwen Luo<sup>1,\*</sup>

<sup>1</sup>Center for Experimental Medicine, The First Affiliated Hospital of Nanchang University, Nanchang, Jiangxi 330006, China

<sup>2</sup>Department of Biochemistry & Molecular Biology, School of Basic Medical Sciences, Nanchang University, Nanchang, Jiangxi 330006, China

<sup>3</sup>State Key Laboratory of Food Science and Technology, Nanchang University, Nanchang, Jiangxi 330047, China

<sup>4</sup>Department of Biostatistics & Epidemiology, School of Public Health, Nanchang University, Nanchang, Jiangxi 330006, China

<sup>5</sup>Department of Hematology, The First Affiliated Hospital of Nanchang University, Nanchang, Jiangxi 330006, China

<sup>6</sup>Department of Molecular Medicine, University of Texas Health Science Center, San Antonio, TX 78229, USA

### Abstract

Focal adhesion kinase (FAK) acts as a regulator of cellular signaling and may promote cell spreading, motility, invasion and survival in malignancy. Elevated expression and activity of FAK frequently correlate with tumor cell metastasis and poor prognosis in breast cancer. However, the mechanisms by which the turnover of FAK is regulated remain elusive. Here we report that heat shock protein 90 $\beta$  (HSP90 $\beta$ ) interacts with FAK and the middle domain (amino acids 233–620) of HSP90 $\beta$  is mainly responsible for this interaction. Furthermore, we found that HSP90 $\beta$  regulates FAK stability since HSP90 $\beta$  inhibitor 17-AAG triggers FAK ubiquitylation and subsequent proteasome-dependent degradation. Moreover, disrupted FAK-HSP90 $\beta$  interaction induced by 17-AAG contributes to attenuation of tumor cell growth, migration, and invasion. Together, our results reveal how HSP90 $\beta$  regulates FAK stability and identifies a potential therapeutic strategy to breast cancer.

© 2014 Elsevier Inc. All rights reserved.

\*To whom correspondence should be addressed: Shiwen Luo, MD & PhD, shiwenluo@ncu.edu.cn, Phone: +86-791-88692139, Fax: +86-791-88623153, 17 Yongwai Street, Donghu District, Nanchang, Jiangxi, 330006, China.

### DISCLOSURE

The authors declare that they have no competing interests as defined by Experimental Cell Research, or other interests that might be perceived to influence the results and discussion reported in this paper.

**Publisher's Disclaimer:** This is a PDF file of an unedited manuscript that has been accepted for publication. As a service to our customers we are providing this early version of the manuscript. The manuscript will undergo copyediting, typesetting, and review of the resulting proof before it is published in its final citable form. Please note that during the production process errors may be discovered which could affect the content, and all legal disclaimers that apply to the journal pertain.

## Keywords

HSP90 $\beta$ ; FAK; breast cancer; metastasis; ubiquitin

---

## INTRODUCTION

Breast cancer is a major cause of morbidity and mortality in women, accounting for 22.9% of the total cancer cases and 13.7% of the cancer deaths (1). Most of the deaths are primarily due to metastasis to distant organs. Metastasis is a multistep process requiring numerous interactions of tumor cells with the surrounding matrix, including adhesion, invasion of basement membrane, survival in circulation, and colonization to a secondary site. Interrupting the metastatic process is key to reducing breast cancer mortality.

Focal adhesion kinase (FAK) is a non-receptor and non-membrane associated protein tyrosine kinase that is activated at the sites of cell-matrix adhesions and integrin clustering by auto-phosphorylation (at Tyr397), Src and other tyrosine kinases (2). FAK controls several cellular signaling pathways, including cell spreading, proliferation, motility, angiogenesis, invasion and survival (3). Elevated FAK levels are detected at early stages of breast cancer tumorigenesis before tumor invasion and metastasis (4, 5). Studies of human breast tumor samples revealed that up-regulation of FAK is observed in 88% of invasive and metastatic tumors, and FAK level correlates with the invasive potential (2, 6). Because of its critical role in the biological processes of cancer cells, FAK has been proposed as a potential target for cancer therapy. Among the FAK inhibitors developed, TAE226, PF562271 and PF573228 are best characterized. TAE226, the first small molecule inhibitor of FAK identified, blocks the ATP binding site and inhibits FAK phosphorylation (7, 8). PF573228 interacts with FAK in its ATP-binding pocket and effectively blocks the catalytic activity of recombinant FAK protein or endogenous FAK expressed in a variety of normal and cancer cell lines (9). Unlike PF573228, PF562271 blocks the ATP binding sites of both FAK and Pyk2 (protein-tyrosine kinase 2) - another non-receptor tyrosine kinase known to bind and activate Src (10, 11). FAK as an anti-cancer target prompts researchers to study related signaling pathways and mechanisms. However, little is known about how FAK interacts with its signaling partners as well as its regulation.

Heat shock protein 90 (HSP90) is an ATPase-directed molecular chaperone that comprises 1–2% of total cellular protein content (12). It has two isoforms, HSP90 $\alpha$  and 90 $\beta$ . HSP90 $\beta$  is slightly larger and less inducible than HSP90 $\alpha$  (13). HSP90 regulates a variety of molecular processes including protein folding, protein degradation, maturation of client proteins, and signal transduction. In cancers, tumor cells rely on HSP90 chaperone machinery to protect an array of mutated and/or over-expressed oncoproteins from misfolding and degradation. Therefore, HSP90 is recognized as a crucial facilitator of oncogene addiction and cancer cell survival (14). Since HSP90 level and activity are up-regulated in cancer cells (15), the effects of the inhibitor of HSP90 on tumorigenesis have been evaluated. Recent studies showed that inhibition of HSP90 by geldanamycin (GA) or 17-(allylamino)-17-demethoxygeldanamycin (17-AAG) leads to apoptosis in various tumor cell types including solid tumors (16, 17).

A large number of HSP90 client proteins have been shown to be pivotal for the development, proliferation and survival of specific types of cancers (18, 19). In the past decades, more than 200 client proteins of HSP90 have been identified (see <http://www.picard.ch/downloads/Hsp90interactors.pdf>). Early work on HSP90 clients mainly focused on two classes: protein kinases and nuclear receptors (20–22). However, as a tyrosine kinase, FAK had not yet been generally considered as a client of HSP90. The relationship of HSP90 and FAK was investigated by limited *in vivo* and *in vitro* studies (23–25). In human studies, enhanced expression of HSP90 and FAK are associated with high risk of transformation and poor survival in acute myeloid leukemia (26). Furthermore, high levels of HSP90 and FAK are predictive of resistance to chemotherapy in acute myeloid leukemia (27, 28). *In vitro*, HSP90 inhibitor GA blocked tyrosine phosphorylation of FAK, assembly of focal adhesions, actin reorganization, and cell migration, all of which were reversed by overexpressing HSP90 in activated HUVEC (29). Pharmacologic inhibition of HSP90 leads to decreased FAK signaling and, consequently, displays growth-inhibitory and anti-metastatic effects similar to FAK inhibition alone in SiHa cervical xenografts (23). Inhibition of cell surface HSP90 suppresses FAK/Src activity and reverses the cell invasion stimulated by FAK overexpression. And FAK knockdown by siRNA treatment in the presence of HSP90 antibody further suppresses invasion of human prostate cancer cell line PC3 (30). However, there is little evidence for the direct interaction between HSP90 and FAK, as well as the consequent effects of the HSP90-FAK interaction on tumorigenesis. Our study focused on the contribution of HSP90 to FAK stability, the HSP90-FAK binding and its functional role in human breast cancer cell. We explored one mechanistic basis for the controlling of cell motility and invasion by FAK in MDA-MB-231 human breast cancer cell. We found that pharmacologic inhibition of HSP90 $\beta$  leads to decreased FAK stability and, as a result, reduced cancer cells growth and metastasis. Moreover, we demonstrated that HSP90 $\beta$  protects FAK from proteasome-mediated degradation.

## MATERIALS AND METHODS

### Reagents, Constructs and Antibodies

Protein-G agarose (11243233001) was obtained from Roche. Glutathione Sepharose 4B (17-0757-01) was from GE Healthcare. Goat anti-mouse IgG conjugated with Alexa Fluor 488 (A21026), goat anti-rabbit IgG conjugated Alexa Fluor 594 (A11012), and blasticidine (R210-01) were from Invitrogen. Recombinant human FAK protein (31168) was from Active Motif (Carlsbad, CA). PF573228 (sc-204179) was from Santa Cruz. U0126 (9903) was from Cell Signaling. Protease inhibitor cocktail (P8340), 17-AAG (A8476), Lubrol-PX, DMSO, and other chemicals were from Sigma (St. Louis, MO). HSP90 $\beta$  miRNAi constructs were generated using the BLOCK-iT Pol II miR RNAi Expression Vector Kit (Invitrogen, K4936-00). Oligonucleotide sequences for miRNAi constructs are 90 $\beta$ -1205 5'-ATA AAG TTG AGG TAC TCA GGT-3' (31), and FAK-1763 5'-ATC ATT TGA AGA CAC CAG AAC-3' (32). A scrambled sequence shRNA that is not homologous to any human gene was used as control. Antibodies were purchased from Santa Cruz (FAK, sc-558; actin, sc-1616), Cell Signaling (p-Tyr397-FAK, 3283S; p-Tyr118-paxillin, 2541; B-Raf, 9434; Raf-1, 9422), Invitrogen (HSP90 $\beta$ , 37-9400; Myc, 132500), Chemicon international (GAPDH, MAB374),

Thermo Scientific (rabbit IgG, 31460; mouse IgG, 31430), Sigma (Flag, F3165; paxillin, P1039).

### Cell Culture and Transfection

MDA-MB-231, HEK293T, and H4 cells were obtained from American Type Culture Collection (ATCC, Manassas) and maintained in DMEM (Gibco) supplemented with 10% fetal bovine serum (FBS) (Invitrogen, Carlsbad, CA), 100 units/ml penicillin G, and 100 µg/ml streptomycin. Cells were incubated in a humidified incubator at 37°C with 5% CO<sub>2</sub>. HEK293T cells were seeded on 10 cm culture dish and allowed to grow till 50–60% confluence, and transfected with the appropriate plasmid using calcium phosphate precipitation methods (33). Forty eight hours after transfection, cells were solubilized in the extraction buffer (0.5% Lubrol-PX, 50 mM KCl, 2 mM CaCl<sub>2</sub>, 20% glycerol, 50 mM Tris-HCl, and inhibitors of proteases and phosphatases, pH 7.4) and subjected to immunoprecipitation and/or immunoblotting. MDA-MB-231 cells were plated in 12-well plates and transfected with the appropriate plasmid using Lipofectamine 2000 (Invitrogen). Six hours after transfection, cells were switched to DMEM containing 10% FBS for 48 h. Then cells were collected, and incubated in selection medium containing 7 µg/ml blasticidine for 2–3 weeks. The stable clones were selected by immunoblotting and immunofluorescence for protein expression.

### Immunoprecipitation, Immunoblotting, and *in vitro* Protein Interaction

Cell lysates were cleaned by centrifugation at 12,000 rpm for 15 min and subjected to immunoprecipitation with indicated antibodies and protein-G beads at 4°C overnight. Bound proteins were resolved by SDS-PAGE and analyzed by immunoblotting as described previously (34, 35). Quantification of immunoblots was done by scanning films containing nonsaturated signals with an Epson 1680 scanner and analyzed with Image J software (31).

The cDNAs encoding full-length HSP90β and HSP90β fragments (1–232, 233–620, 621–724) were sub-cloned into the pGEX-6P-1 vector. Expression of GST-HSP90β, GST-HSP90β fragments or GST alone was conducted in the protease-deficient bacterial strain *E. coli* BL21 (DE3). Protein expression was induced for 6–8 h at 25°C with 0.4 mM isopropyl β-D-thiogalactopyranoside. GST and GST fusion proteins were purified by glutathione sepharose 4B beads, and incubated with lysates of HEK293T cells expressing Myc-FAK at 4°C overnight. The beads were collected, and the fusion proteins were probed with anti-Myc antibody by Western blotting.

### Cell Migration and Colony Formation Assays

Cell migration was measured by a scratch assay (36). MDA-MB-231 cells were plated in 6-well plates to create a confluent monolayer after a 12 h culture at 37°C in an incubator with 5% CO<sub>2</sub>. Then, a p200 pipette tip was used to create a “scratch” in the cell monolayer. After removing debris and adding fresh media containing 2% FBS, cells were photographed using converted fluorescence microscope (Olympus, IX71) at 0, 12, 18 and 24 h in the presence or absence of 17-AAG or PF573228. The wound area was assessed by ImageJ software. A relative migration rate was calculated by cell relative migration rate for each treatment.

Colony formation was assessed using a soft agar assay (37). Briefly, cells were suspended in DMEM containing 0.33% agarose and 10% fetal bovine serum and plated on top of a solidified layer of DMEM containing 0.67% agarose and 10% fetal bovine serum. The cells were plated at a density of 1,000 cells/well in a 12-well plate and fed weekly by adding 1 ml of conditioned DMEM containing 0.33% agarose and 10% fetal bovine serum. After 18–21 days of growth, colonies of >50 cells were scored. The efficiency of colony formation was determined by counting the number of colonies and calculated as the following: (number of colonies formed/number of cells plated)  $\times$  100% (38).

### Cell Invasion Assay

Cell invasion assay was performed in a 24-well transwell chamber (Corning, Inc., Corning, NY). The 8  $\mu$ m pore polycarbonate membrane insert was coated with 100  $\mu$ l of matrigel (BD Biosciences). The matrigel was diluted to 100  $\mu$ g/ml with cold DMEM, and applied to the upper surface of the Inserts (5  $\mu$ g/Insert), then dried overnight under a hood at room temperature. Cells ( $2 \times 10^5$  cells/ml) with or without 17-AAG or PF573228 were plated to the upper chamber, and 700  $\mu$ l of 10% FBS medium were placed in the bottom chamber. After incubation at 37°C for 24 h, the upper surface of the insert was swabbed to remove non-migrating cells. The inserts were washed with PBS, fixed in 4% paraformaldehyde and stained with crystal violet for 30 min. Photographs were taken and stained cells were counted under a microscope in five randomly chosen fields and presented as percentage of the control.

### Immunofluorescent Analysis

Cells were grown on coverslips in 12-well plates and fixed with 4% paraformaldehyde for 20 min at room temperature. Cells were permeabilized with 0.1% Triton X-100 in PBS for 10 min and blocked with 10% BSA in PBS for 60 min, and then stained with the indicated antibodies. Double-labelled immunostaining was done with appropriate fluorochrome-conjugated secondary antibodies. Images were taken using confocal microscope (Zeiss, LSM 700). For F-actin staining, cells were placed on glass coverslips in a 12-well culture plate at  $10 \times 10^4$  cells/well. The next day cells were treated with 17-AAG or PF573228 for 16 h, and then fixed with 3.7% formaldehyde. Glass coverslips were removed from the plate and cells were permeabilized with 0.1% Triton X-100 for 3 min and immediately washed twice in PBS. Coverslips were blocked with 1% BSA for 30 min, and then replaced with Alexa Fluor® 488 phalloidin (Invitrogen, A12379) containing 1% BSA for 20 min at room temperature. After washed with PBS, coverslips were air dried and mounted on a microscope slide. Representative photographs were taken using confocal microscope (Zeiss, LSM 700).

### Statistical Analyses

Each assay was repeated three times. Data are expressed as the mean  $\pm$  standard deviation (SD). The statistical significance of the data obtained was evaluated using the Student's *t*-test. Statistical significance was defined as  $P < 0.05$ .

## RESULTS

### HSP90 $\beta$ Interacts with FAK in Mammalian Cells

Although the impact of HSP90 on FAK has been investigated by several studies, none of them provides evidence of direct binding of these two proteins. To evaluate whether HSP90 $\beta$  protein interacts with FAK, we transfected Myc-tagged FAK and Flag-tagged HSP90 $\beta$  into HEK293T cells. As shown in Figure 1A, Flag-HSP90 $\beta$  was detected in immunoprecipitates of Myc-FAK, suggesting an interaction between FAK and HSP90 $\beta$ . To confirm that endogenous FAK indeed binds to HSP90 $\beta$ , the immunoprecipitation experiment was carried out with the endogenous proteins isolated from MDA-MB-231 breast cancer cells. We found that endogenous FAK was immunoprecipitated with endogenous HSP90 $\beta$  (Figure 1B). To further assess if this interaction was direct, we performed *in vitro* GST pull-down assay using GST-HSP90 $\beta$  and recombinant human FAK protein. The complex was detected by immunoblotting analysis (Figure 1C), suggesting a direct interaction between HSP90 $\beta$  and FAK. In addition, immunofluorescence studies by confocal microscopy revealed intense staining of FAK in nuclei while scattered in cytoplasm (Figure 1D). However, HSP90 $\beta$  was found hyperchromatic in the cytoplasm as well as at the rim of cell lamellipodia, and markedly co-stained with FAK outside the nuclei. We found similar distribution of these two proteins in H4 neuronal glioma cells, which have relatively bigger nuclei and less cytoplasm than MDA-MB-231 cells. Furthermore, as shown in Figure 1E, the immunoprecipitation assay of HSP90 co-chaperones (HSP70, HSP40, HOP) and FAK indicates the possible binding between FAK and other HSP90 $\beta$  partners.

### Domains of HSP90 $\beta$ Crucial for Interaction with FAK

Since the results above demonstrated the interaction between HSP90 $\beta$  and FAK, we wondered which domain is responsible for the binding. HSP90 is known to be composed of three major structural domains: the nucleotide binding domain in the N-terminal portion which contains the ATP-binding site; the client binding domain in the middle; and a C-terminal domain responsible for HSP90 dimerization. To determine the domain(s) responsible for the interaction with FAK, we obtained a series of HSP90 $\beta$  deletion mutants. Plasmids bearing Myc-tagged FAK and Flag-tagged HSP90 $\beta$  derivatives were transiently cotransfected into HEK293T cells. Lysates were immunoprecipitated with antibody against Myc (Figure 2A, middle). Myc-FAK was able to co-immunoprecipitate with HSP90 $\beta$  full length and truncation mutants 1–439, 1–620, 440–620, 233–439, but failed to immunoprecipitate with 1–232, suggesting that the middle domain of HSP90 $\beta$  is the main region for the interaction with FAK (Figure 2A, B). Note that truncation mutants of 440–620 and 233–439 interacted with FAK, suggesting at least two binding sites in the middle domain responsible for the binding (Figure 2A, B). Moreover, GST fusion protein of HSP90 $\beta$  containing 233–620 strongly interacts with Myc-tagged FAK generated by *in vitro* translation (Figure 2C, D). The results indicate that the middle domain of HSP90 accounts for the majority of FAK-binding and two regions (i.e., 1–232, 627–724) also contribute to the interaction with FAK.



## HSP90 $\beta$ Protects FAK from Degradation through Ubiquitin-proteasome Pathway

The binding of HSP90 $\beta$  to FAK prompted us to investigate the function of HSP90 $\beta$  in FAK stability. MDA-MB-231 cells were treated with 17-AAG, an inhibitor that competes with ATP for binding to the N-terminal HSP90 (39). Cycloheximide (CHX) was used to inhibit protein synthesis for monitoring protein degradation. As shown in Figure 3A, endogenous FAK is degraded slowly under normal condition, however, 17-AAG markedly accelerated FAK turnover during 16 h observation. Quantification analysis confirmed the significant difference between these two groups (Control group:  $79.62 \pm 5.31\%$  vs 17-AAG group:  $52.14 \pm 4.61\%$  at 16 h,  $P < 0.01$ ) (Figure 3B).

Degradation of HSP90 client proteins is thought to be mediated by the 26S proteasome (31). Therefore, we investigated whether the proteasome is involved in regulating FAK stability. MDA-MB-231 cells were treated with MG-132, an inhibitor of the 26S proteasome. As shown in Figure 3C, the degradation of FAK induced by 17-AAG was attenuated partially when MG-132 was added for 4 h and 8 h. These results suggest that FAK undergoes rapid degradation by 26S proteasomes without the protection of HSP90 $\beta$ .

Polyubiquitinated proteins are substrates for the 26S proteasome (40). To further investigate effects of HSP90 $\beta$  on ubiquitin-dependent degradation of FAK, MDA-MB-231 cells were treated with 17-AAG alone or together with MG-132 for 4 h and 8 h incubation prior to cell collection. Lysates were immunoprecipitated with FAK and the immunoprecipitates were probed for ubiquitin (Figure 3D). Lane 1 showed a basal ubiquitination profile of FAK under normal condition (Figure 3D, lane 1), and 17-AAG enhanced FAK ubiquitination slightly (Figure 3D, lane 2). MG-132 treatment in the absence of 17-AAG resulted in significant accumulation of ubiquitinated FAK, confirming ubiquitin/proteasome-mediated FAK degradation (Figure 3D, lane 5, 6). 17-AAG enhanced FAK ubiquitination markedly with the combination of MG-132 treatment in comparison with vehicle control (Figure 3D, lane 3, 4).

Next, we adopted a dominant-negative approach to further investigate the interaction of HSP90 $\beta$  and FAK. We reasoned that HSP90 $\beta$ (1–620), a fragment that contains the domain for FAK interaction, may prevent endogenous FAK from interacting with HSP90 $\beta$ . As shown in Figure 3E, expression of Flag-HSP90 $\beta$ (1–620) reduced expression of endogenous FAK in HEK293T cells, indicating a disrupted interaction between FAK and endogenous HSP90 $\beta$  as a result of competitive binding between HSP90 $\beta$ (1–620) and FAK. These data strongly suggest that HSP90 $\beta$  plays a critical role in FAK stability, likely by means of inhibiting proteasome-dependent degradation of FAK.

## Inhibition of HSP90 $\beta$ or FAK Attenuates Tumorigenesis of Breast Cancer Cells

To explore possible functional effects of HSP90 $\beta$  on the role of FAK in tumorigenesis, we used MDA-MB-231 cells to perform scratch assays. Cells were pretreated with PF573228 or 17-AAG to inhibit FAK and HSP90 $\beta$  respectively, before wounded by scratching. After additional 12, 18, and 24 h incubation, repopulation of the open area created by the “scratch” was markedly reduced in PF573228- and 17-AAG-treated cells compared with non-treated control cells (Figure 4A, B). Further quantification analysis showed a dose-

dependent inhibition. In a transwell assay, PF573228- and 17-AAG-treated cells exhibited reduced cell invasive ability when compared to untreated cells (Figure 4C, D). Consistently, in anchorage-independent growth assay (Figure 4E and 4F), PF573228 and 17-AAG inhibited MDA-MB-231 cells colony formation compared with solvent-treated control cells.

To evaluate the specificity of biochemical effect of the HSP90 $\beta$ -FAK interaction, we presented data of other HSP90 client proteins B-Raf and Raf-1 (C-Raf) that are components of the Ras/Raf/MEK/ERK signaling module, an FAK-independent pathway that regulates cell fate (41, 42). As shown in Supplemental Figure S1A, 17-AAG exposure led to diminished expression of FAK, B-Raf and Raf-1 to different extent. U0126, an MEK1/2 inhibitor, was employed to block the B-Raf and Raf-1 pathway in scratch assay and transwell assay using MDA-MB-231 cells (Supplemental Figure S1B and S1C). There are no significant difference between U0126-treated and control cells, supporting the specific effect of FAK-HSP90 in tumorigenesis of breast cancer cells. From the above, inhibition of FAK or HSP90 $\beta$  was found to similarly regulate tumor cell growth, invasion and metastasis. FAK and HSP90 $\beta$  likely work together since FAK interacts with HSP90 $\beta$ .

### **Repression of FAK and HSP90 $\beta$ Expression Inhibits Cell Migration and Anchorage-independent Growth**

To further assess specific roles of HSP90 $\beta$  and FAK in breast cancer, we generated FAK and HSP90 $\beta$  miRNAi constructs that inhibited FAK and HSP90 $\beta$  expression, respectively. We screened several stable cell lines for knockdown of FAK or HSP90 $\beta$ . As shown by immunoblottings, 3 of 4 cell lines (FAK1763-#1, #3, #4) transfected with miRNAi-FAK1763 (miR-FAK1763) and all of the 3 cell lines (90 $\beta$ -1205-#1, #2, #3) transfected with miRNAi-90 $\beta$ -1205 (miR-90 $\beta$ -1205) exhibited lower expression of FAK and HSP90 $\beta$  respectively, than control cells bearing a vector with random sequences (Figure 5A, B). Scratch assays showed that repopulation of the open area created by the “scratch” was markedly attenuated when MDA-MB-231 cells were transfected with either miR-FAK1763 or miR-90 $\beta$ -1205 (Figure 5C, D). However, transient suppression of Raf-1 by siR-Raf-1 (Supplemental Figure S2A) did not affect cell migration and invasion of MDA-MB-231 cells (Supplemental Figure S2B and S2C). In anchorage-independent growth assay, FAK and HSP90 $\beta$  knockdown cells formed fewer colonies on soft agar than control cells (Figure 5E, F). Together these results established that FAK is stabilized by HSP90 $\beta$ , and the interaction between HSP90 $\beta$  and FAK plays an essential role in breast cancer cell metastasis and transformation.

### **Inhibition of HSP90 $\beta$ or FAK Interferes Invasive Ability and Cytoskeleton of Tumor Cells**

Next, we further addressed the effect of HSP90 $\beta$  or FAK on tumor cell invasion and cytoskeletal reorganization. Like FAK, its downstream target paxillin is a positive regulator of cell adhesion and migration. Paxillin serves as a platform for the recruitment of numerous regulatory and structural proteins that together control the dynamic changes in cell adhesion, cytoskeletal reorganization and gene expression that are necessary for cell migration and survival (43). 17-AAG reduced expression of paxillin slightly, but diminished phosphorylation form of paxillin (p-paxillin) drastically (Figure 6A). Cytoskeleton was visualized by immunofluorescent staining of actin in PF573228- or 17-AAG-treated MDA-



MB-231 and H4 neuroglioma cells. As shown in Figure 6B, normally, cells displayed polarized leading edges rich in actin ruffles, and exhibited numerous and thick stress fibers. However, PF573228 and 17-AAG treatment inhibited actin ruffling at the leading edge of MDA-MB-231 cells, accompanied by thinner and less stress fibers than those observed in control cells. Although the actin of PF573228- and 17-AAG- treated H4 cells were stained intensely at the edges, they usually lacked well-developed polarized leading edges. Congruously, all the cytoplasm of treated cells was filled with fractured debris of stress fibers. These results demonstrate a requirement of FAK and HSP90 $\beta$  for breast cancer cell motility.

Based on the results we obtained, we propose a working hypothesis depicted in Figure 6C. According to this model, in MDA-MB-231 cells, HSP90 $\beta$  normally interacts with FAK to form a stable complex, thus ensures the functions of FAK in promoting tumorigenesis. When HSP90 $\beta$  activity is blocked by 17-AAG, FAK undergoes proteasome-dependent degradation, resulting in prevention of tumor cell migration and invasion.

## DISCUSSION

Our study has demonstrated a novel finding that HSP90 $\beta$  stabilizes FAK through protein-protein interaction in MDA-MB-231 breast cancer cells, otherwise, FAK encounters proteasome-dependent degradation when treated with HSP90 $\beta$  inhibitor 17-AAG. We show that HSP90 $\beta$  regulates FAK stability based on three important findings. First, both ectopically expressed and endogenous HSP90 $\beta$  directly interact with FAK in mammalian cells. Under confocal microscopy, overlapped fluorescent staining of HSP90 $\beta$  and FAK can be observed. Second, treatment of MDA-MB-231 cells with HSP90 inhibitor 17-AAG results in accelerated degradation of FAK protein. Third, disruption of the HSP90 $\beta$ -FAK interaction by a dominant-negative approach reduces endogenous FAK level. Our data suggest a novel regulatory mechanism for FAK in tumor cells as HSP90 $\beta$  protects FAK from proteasome-dependent degradation.

FAK has been reported to be overexpressed in several cancer types, including tumors derived from the breast, cervix, head and neck, thyroid, colon and ovary (6, 44–46). However, noninvasive, hypercellular neoplastic tissues such as parathyroid and hepatocellular adenomas do not contain elevated FAK (6). Therefore, FAK has been proposed as a potential target for diagnosis and therapy in malignant cancer. Published reports have implicated both HSP90 $\beta$  and FAK in the development/progression of cancer, as their expressions are detectable in many epithelial tumors or patients' serum and are associated with unfavorable clinical outcome (2, 6, 26, 27). However, limited data support the involvement of HSP90 $\beta$  in FAK signaling (47), and the regulatory role of HSP90 $\beta$  on FAK stability has been unclear (23). Ochel HJ, et al. revealed that GA stimulates the proteolytic degradation of FAK in several cancer cell lines including breast cancer cell, and markedly reduces the half-life of newly synthesized FAK protein without altering the level of FAK mRNA (47). Our data by using GA clinical derivative 17-AAG update that study and provide additional new findings. We present direct evidence for the HSP90-FAK interaction as exogenous HSP90 $\beta$  immunoprecipitated with FAK in HEK293T cells, which is consistent with results from co-immunoprecipitation of endogenous HSP90 $\beta$  and FAK in

MDA-MB-231 cells (Figure 1A,1B). Our data also reveal that the co-chaperones of HSP90 $\beta$ -HOP, HSP70, and HSP40 interact with FAK by co-immunoprecipitation, suggesting that HSP90 does not act alone in FAK regulation, but likely requires the aid of several co-chaperone proteins.

Moreover, we demonstrated that the main binding site(s) of HSP90 $\beta$  to FAK is in the middle region, which is known for client engagement (48). Notably, although it is reported that HSP90 mostly resides in cytoplasm, sometimes HSP90 is also found to be expressed on cell surface in cancer cells. In our study, cell surface HSP90 was localized at the leading edge of lamellipodia which is associated with migrating ability of breast cancer cells (Figure 1D), suggesting that it may play a critical role in form of complex with FAK in cell motility. However, whether cell surface HSP90 interacts with FAK locally or cytosolic HSP90 is recruited by FAK related signaling to the rim of lamellipodia is still under investigation.

Several HSP90 inhibitors are currently being evaluated for anti-cancer activity in numerous Phase II and several Phase III clinical trials, both as single agent and in combination with other cancer drugs (49, 50). Since oncogenes rely heavily on HSP90 to chaperone their conformation and the inhibitor of HSP90 is able to affect multiple targets and pathways, HSP90 inhibitors can play a unique role in preventing drug resistance in tumors. However, because of the overwhelming targets of HSP90, tissue toxicity, and the harmful solvent of 17-AAG, ongoing clinical trials revealed various suggestive maximal tolerated doses and administration schedules of 17-AAG (51–55). In addition, the data from most phase I clinical trials with monotherapy of 17-AAG indicated a minor objective anti-tumor response. Therefore, other derivatives of GA and water soluble HSP90 inhibitors are required. We aim to find new client protein of HSP90 associated with tumorigenesis and mechanism of their interaction, thus provide potential agents in combination with HSP90 inhibitors. The pharmacological inhibitor of FAK, PF573228, exhibits similar inhibitory effects as 17-AAG on tumor cell growth, metastasis and motility. Small molecule inhibitors of FAK (e.g., PF-562271, PF-04554878 and GSK2256098, etc.) are already in clinical testing, and the first FAK inhibitor PF562271 was tested in clinical Phase I trial (56). Our results support further studies of FAK as a promising therapeutic target.

In summary, this study provides critical insights into the role of HSP90 $\beta$  in FAK stabilization, and proteasome-dependent degradation of FAK without conformational protection of HSP90. The direct binding with HSP90 $\beta$  demonstrated that FAK should be a new oncogenic client of HSP90. Furthermore, breast cancer cells treated with inhibitors of FAK or HSP90 $\beta$  exhibit decreased cell growth and metastasis, which provides a novel pathway that may contribute to treating tumors. Together, our results reveal how HSP90 $\beta$  regulates FAK stability and provided a new potential therapeutic strategy to alleviate breast cancer.

## Supplementary Material

Refer to Web version on PubMed Central for supplementary material.

## Acknowledgments

We thank Dr. Subrata Haldar (University of Texas) for editorial assistance of this manuscript, Dr. Lin Mei (Georgia Regents University) for HSP90 constructs, Dr. Zhijun Luo (Nanchang University) for reagents and Ms. Lingfang Wang for assistance with imaging analysis. This work was supported in part by grants from the China National Basic Research Program (2010CB535001), the National Natural Science Foundation of China (81060095, 31171359), the Program of International S&T Cooperation Projects of China (010S2012ZR02), the Natural Science Foundation of Jiangxi Province (20114BAB205035 and 20132BAB205109) and the NIH (P30 CA054174).

## REFERENCES

1. Ferlay J, et al. Estimates of worldwide burden of cancer in 2008: GLOBOCAN 2008. *International journal of cancer. Journal international du cancer*. 2010; 127:2893–2917. [PubMed: 21351269]
2. McLean GW, et al. The role of focal-adhesion kinase in cancer - a new therapeutic opportunity. *Nature reviews. Cancer*. 2005; 5:505–515.
3. Hanks SK, Ryzhova L, Shin NY, Brabek J. Focal adhesion kinase signaling activities and their implications in the control of cell survival and motility. *Frontiers in bioscience : a journal and virtual library*. 2003; 8:d982–996. [PubMed: 12700132]
4. Cance WG, et al. Immunohistochemical analyses of focal adhesion kinase expression in benign and malignant human breast and colon tissues: correlation with preinvasive and invasive phenotypes. *Clinical cancer research : an official journal of the American Association for Cancer Research*. 2000; 6:2417–2423. [PubMed: 10873094]
5. Lightfoot HM Jr, et al. Upregulation of focal adhesion kinase (FAK) expression in ductal carcinoma in situ (DCIS) is an early event in breast tumorigenesis. *Breast cancer research and treatment*. 2004; 88:109–116. [PubMed: 15564794]
6. Owens LV, et al. Overexpression of the focal adhesion kinase (p125FAK) in invasive human tumors. *Cancer research*. 1995; 55:2752–2755. [PubMed: 7796399]
7. Halder J, et al. Therapeutic efficacy of a novel focal adhesion kinase inhibitor TAE226 in ovarian carcinoma. *Cancer research*. 2007; 67:10976–10983. [PubMed: 18006843]
8. Liu TJ, et al. Inhibition of both focal adhesion kinase and insulin-like growth factor-I receptor kinase suppresses glioma proliferation in vitro and in vivo. *Molecular cancer therapeutics*. 2007; 6:1357–1367. [PubMed: 17431114]
9. Slack-Davis JK, et al. Cellular characterization of a novel focal adhesion kinase inhibitor. *The Journal of biological chemistry*. 2007; 282:14845–14852. [PubMed: 17395594]
10. Bagi CM, Roberts GW, Andresen CJ. Dual focal adhesion kinase/Pyk2 inhibitor has positive effects on bone tumors: implications for bone metastases. *Cancer*. 2008; 112:2313–2321. [PubMed: 18348298]
11. Roberts WG, et al. Antitumor activity and pharmacology of a selective focal adhesion kinase inhibitor, PF-562,271. *Cancer research*. 2008; 68:1935–1944. [PubMed: 18339875]
12. Young JC, Hartl FU. Polypeptide release by Hsp90 involves ATP hydrolysis and is enhanced by the co-chaperone p23. *The EMBO journal*. 2000; 19:5930–5940. [PubMed: 11060043]
13. Csermely P, Schnaider T, Soti C, Prohászka Z, Nardai G. The 90-kDa molecular chaperone family: structure, function, and clinical applications. A comprehensive review. *Pharmacology & therapeutics*. 1998; 79:129–168. [PubMed: 9749880]
14. Whitesell L, Lindquist SL. HSP90 and the chaperoning of cancer. *Nature reviews. Cancer*. 2005; 5:761–772.
15. Kamal A, et al. A high-affinity conformation of Hsp90 confers tumour selectivity on Hsp90 inhibitors. *Nature*. 2003; 425:407–410. [PubMed: 14508491]
16. Karkoulis PK, Stravopodis DJ, Konstantakou EG, Voutsinas GE. Targeted inhibition of heat shock protein 90 disrupts multiple oncogenic signaling pathways, thus inducing cell cycle arrest and programmed cell death in human urinary bladder cancer cell lines. *Cancer cell international*. 2013; 13:11. [PubMed: 23394616]
17. Georgakis GV, et al. Inhibition of heat shock protein 90 function by 17-allylamino-17-demethoxygeldanamycin in Hodgkin's lymphoma cells down-regulates Akt kinase, dephosphorylates extracellular signal-regulated kinase, and induces cell cycle arrest and cell death. *Clinical cancer*

- research : an official journal of the American Association for Cancer Research. 2006; 12:584–590. [PubMed: 16428504]
18. Solit DB, Rosen N. Hsp90: a novel target for cancer therapy. *Current topics in medicinal chemistry*. 2006; 6:1205–1214. [PubMed: 16842157]
  19. Taipale M, Jarosz DF, Lindquist S. HSP90 at the hub of protein homeostasis: emerging mechanistic insights. *Nature reviews. Molecular cell biology*. 2010; 11:515–528.
  20. Ziemiecki A, Catelli MG, Joab I, Moncharmont B. Association of the heat shock protein hsp90 with steroid hormone receptors and tyrosine kinase oncogene products. *Biochemical and biophysical research communications*. 1986; 138:1298–1307. [PubMed: 3530253]
  21. Howard KJ, Holley SJ, Yamamoto KR, Distelhorst CW. Mapping the HSP90 binding region of the glucocorticoid receptor. *The Journal of biological chemistry*. 1990; 265:11928–11935. [PubMed: 2365707]
  22. Xu Y, Lindquist S. Heat-shock protein hsp90 governs the activity of pp60v-src kinase. *Proceedings of the National Academy of Sciences of the United States of America*. 1993; 90:7074–7078. [PubMed: 7688470]
  23. Schwock J, et al. Targeting focal adhesion kinase with dominant-negative FRNK or Hsp90 inhibitor 17-DMAG suppresses tumor growth and metastasis of SiHa cervical xenografts. *Cancer research*. 2009; 69:4750–4759. [PubMed: 19458065]
  24. Masson-Gadais B, Houle F, Laferriere J, Huot J. Integrin alphavbeta3, requirement for VEGFR2-mediated activation of SAPK2/p38 and for Hsp90-dependent phosphorylation of focal adhesion kinase in endothelial cells activated by VEGF. *Cell stress & chaperones*. 2003; 8:37–52. [PubMed: 12820653]
  25. Le Boeuf F, Houle F, Huot J. Regulation of vascular endothelial growth factor receptor 2-mediated phosphorylation of focal adhesion kinase by heat shock protein 90 and Src kinase activities. *The Journal of biological chemistry*. 2004; 279:39175–39185. [PubMed: 15247219]
  26. Flandrin-Gresta P, et al. Heat Shock Protein 90 is overexpressed in high-risk myelodysplastic syndromes and associated with higher expression and activation of Focal Adhesion Kinase. *Oncotarget*. 2012; 3:1158–1168. [PubMed: 23047954]
  27. Flandrin P, et al. Significance of heat-shock protein (HSP) 90 expression in acute myeloid leukemia cells. *Cell stress & chaperones*. 2008; 13:357–364. [PubMed: 18386162]
  28. Kornblau SM, et al. Simultaneous activation of multiple signal transduction pathways confers poor prognosis in acute myelogenous leukemia. *Blood*. 2006; 108:2358–2365. [PubMed: 16763210]
  29. Rousseau S, et al. Vascular endothelial growth factor (VEGF)-driven actin-based motility is mediated by VEGFR2 and requires concerted activation of stress-activated protein kinase 2 (SAPK2/p38) and geldanamycin-sensitive phosphorylation of focal adhesion kinase. *The Journal of biological chemistry*. 2000; 275:10661–10672. [PubMed: 10744763]
  30. Liu X, et al. Cell surface heat shock protein 90 modulates prostate cancer cell adhesion and invasion through the integrin-beta1/focal adhesion kinase/c-Src signaling pathway. *Oncology reports*. 2011; 25:1343–1351. [PubMed: 21369706]
  31. Luo S, et al. HSP90 beta regulates rapsyn turnover and subsequent AChR cluster formation and maintenance. *Neuron*. 2008; 60:97–110. [PubMed: 18940591]
  32. Luo SW, et al. Regulation of heterochromatin remodelling and myogenin expression during muscle differentiation by FAK interaction with MBD2. *The EMBO journal*. 2009; 28:2568–2582. [PubMed: 19661918]
  33. Graham FL, van der Eb AJ. A new technique for the assay of infectivity of human adenovirus 5 DNA. *Virology*. 1973; 52:456–467. [PubMed: 4705382]
  34. Luo ZG, et al. Regulation of AChR clustering by Dishevelled interacting with MuSK and PAK1. *Neuron*. 2002; 35:489–505. [PubMed: 12165471]
  35. Zhu D, Xiong WC, Mei L. Lipid rafts serve as a signaling platform for nicotinic acetylcholine receptor clustering. *The Journal of neuroscience : the official journal of the Society for Neuroscience*. 2006; 26:4841–4851. [PubMed: 16672658]
  36. Liang CC, Park AY, Guan JL. In vitro scratch assay: a convenient and inexpensive method for analysis of cell migration in vitro. *Nature protocols*. 2007; 2:329–333.

37. Wang JB, Wu WJ, Cerione RA. Cdc42 and Ras cooperate to mediate cellular transformation by intersectin-L. *The Journal of biological chemistry*. 2005; 280:22883–22891. [PubMed: 15824104]
38. Ratliff TL, Kadmon D, Shapiro A, Jacobs AJ, Heston WD. Inhibition of mouse bladder tumor proliferation by murine interferon-gamma and its synergism with interferon-beta. *Cancer research*. 1984; 44:4377–4381. [PubMed: 6432311]
39. Sharp S, Workman P. Inhibitors of the HSP90 molecular chaperone: current status. *Advances in cancer research*. 2006; 95:323–348. [PubMed: 16860662]
40. Spataro V, Norbury C, Harris AL. The ubiquitin-proteasome pathway in cancer. *British journal of cancer*. 1998; 77:448–455. [PubMed: 9472642]
41. Wellbrock C, Karasarides M, Marais R. The RAF proteins take centre stage. *Nature reviews. Molecular cell biology*. 2004; 5:875–885.
42. da Rocha Dias S, et al. Activated B-RAF is an Hsp90 client protein that is targeted by the anticancer drug 17-allylamino-17-demethoxygeldanamycin. *Cancer research*. 2005; 65:10686–10691. [PubMed: 16322212]
43. Deakin NO, Turner CE. Paxillin comes of age. *Journal of cell science*. 2008; 121:2435–2444. [PubMed: 18650496]
44. Oktay MH, Oktay K, Hamele-Bena D, Buyuk A, Koss LG. Focal adhesion kinase as a marker of malignant phenotype in breast and cervical carcinomas. *Human pathology*. 2003; 34:240–245. [PubMed: 12673558]
45. Kornberg LJ. Focal adhesion kinase and its potential involvement in tumor invasion and metastasis. *Head & neck*. 1998; 20:745–752. [PubMed: 9790298]
46. Judson PL, He X, Cance WG, Van Le L. Overexpression of focal adhesion kinase, a protein tyrosine kinase, in ovarian carcinoma. *Cancer*. 1999; 86:1551–1556. [PubMed: 10526262]
47. Ochel HJ, Schulte TW, Nguyen P, Trepel J, Neckers L. The benzoquinone ansamycin geldanamycin stimulates proteolytic degradation of focal adhesion kinase. *Molecular genetics and metabolism*. 1999; 66:24–30. [PubMed: 9973544]
48. Meyer P, et al. Structural basis for recruitment of the ATPase activator Aha1 to the Hsp90 chaperone machinery. *The EMBO journal*. 2004; 23:1402–1410. [PubMed: 15039704]
49. Workman P, Burrows F, Neckers L, Rosen N. Drugging the cancer chaperone HSP90: combinatorial therapeutic exploitation of oncogene addiction and tumor stress. *Annals of the New York Academy of Sciences*. 2007; 1113:202–216. [PubMed: 17513464]
50. Taldone T, Gozman A, Maharaj R, Chiosis G. Targeting Hsp90: small-molecule inhibitors and their clinical development. *Current opinion in pharmacology*. 2008; 8:370–374. [PubMed: 18644253]
51. Goetz MP, et al. Phase I trial of 17-allylamino-17-demethoxygeldanamycin in patients with advanced cancer. *Journal of clinical oncology : official journal of the American Society of Clinical Oncology*. 2005; 23:1078–1087. [PubMed: 15718306]
52. Banerji U, et al. Phase I pharmacokinetic and pharmacodynamic study of 17-allylamino, 17-demethoxygeldanamycin in patients with advanced malignancies. *Journal of clinical oncology : official journal of the American Society of Clinical Oncology*. 2005; 23:4152–4161. [PubMed: 15961763]
53. Ramanathan RK, et al. Phase I pharmacokinetic-pharmacodynamic study of 17-(allylamino)-17-demethoxygeldanamycin (17AAG, NSC 330507), a novel inhibitor of heat shock protein 90, in patients with refractory advanced cancers. *Clinical cancer research : an official journal of the American Association for Cancer Research*. 2005; 11:3385–3391. [PubMed: 15867239]
54. Grem JL, et al. Phase I and pharmacologic study of 17-(allylamino)-17-demethoxygeldanamycin in adult patients with solid tumors. *Journal of clinical oncology : official journal of the American Society of Clinical Oncology*. 2005; 23:1885–1893. [PubMed: 15774780]
55. Solit DB, et al. Phase I trial of 17-allylamino-17-demethoxygeldanamycin in patients with advanced cancer. *Clinical cancer research : an official journal of the American Association for Cancer Research*. 2007; 13:1775–1782. [PubMed: 17363532]
56. Infante JR, et al. Safety, pharmacokinetic, and pharmacodynamic phase I dose-escalation trial of PF-00562271, an inhibitor of focal adhesion kinase, in advanced solid tumors. *Journal of clinical*

oncology : official journal of the American Society of Clinical Oncology. 2012; 30:1527–1533.  
[PubMed: 22454420]



**Highlights**

- HSP90 $\beta$  protects FAK from degradation by the ubiquitin-proteasome pathway.
- Inhibition of HSP90 $\beta$  or FAK attenuates tumorigenesis of breast cancer cells.
- Genetic repression of HSP90 $\beta$  or FAK inhibits tumor cell migration and proliferation.
- Inhibition of HSP90 $\beta$  or FAK interferes cell invasion and cytoskeleton.

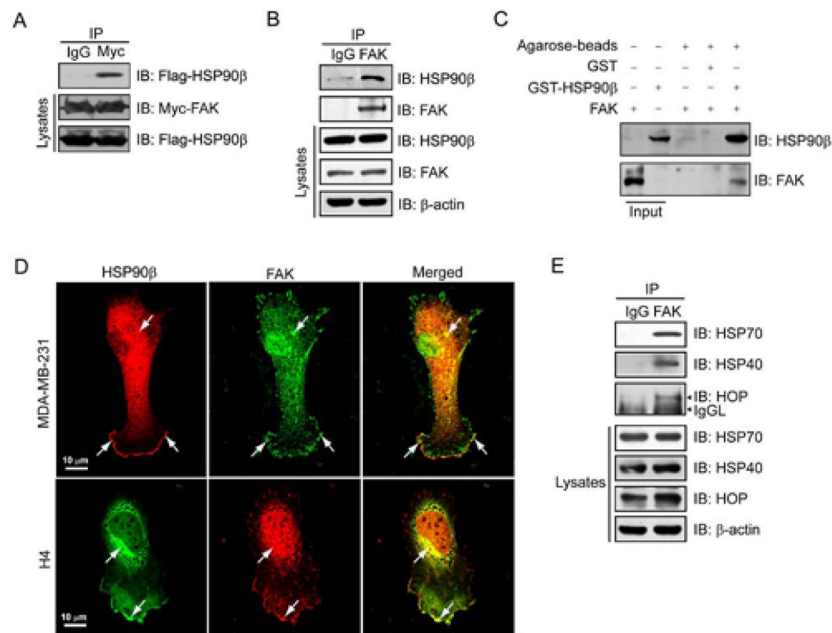


**Figure 1.**

Interaction between FAK and HSP90 $\beta$  in cultured cells. (A) Co-immunoprecipitation of exogenously transfected HSP90 $\beta$  with transfected FAK in cultured HEK293T cells. Cells were transfected with Flag-HSP90 $\beta$  and Myc-FAK plasmids. Forty-eight hours after transfection, cell lysates were incubated with antibodies against Myc or rabbit normal IgG as control to immunoprecipitate FAK complexes, which were subsequently resolved on SDS-PAGE and immunoblotted with antibodies against Flag. The levels of Myc-tagged FAK and Flag-tagged HSP90 $\beta$  in lysates were assessed by immunoblotting with anti-Myc and anti-Flag antibodies, respectively. (B) Interaction of FAK with HSP90 $\beta$  in MDA-MB-231 cells by co-immunoprecipitation assay. Precipitates and the lysates were probed for HSP90 $\beta$  and FAK. (C) Direct interaction between FAK and HSP90 was confirmed *in vitro* by GST pull-down assay. (D) Colocalization of HSP90 $\beta$  and FAK in MDA-MB-231 and H4 cells. The samples were fixed and co-stained with antibodies against HSP90 $\beta$  (Alexa Fluor 488, green) and FAK (Alexa Fluor 594, red). Images were acquired by using a Zeiss confocal microscope. Arrows indicate colocalization. Scale bar, 10  $\mu$ m. (E) Immunoprecipitation assay of endogenous FAK and HSP90 co-chaperones. Immunoprecipitates and the lysates were probed for HSP70, HSP40, HOP and FAK.

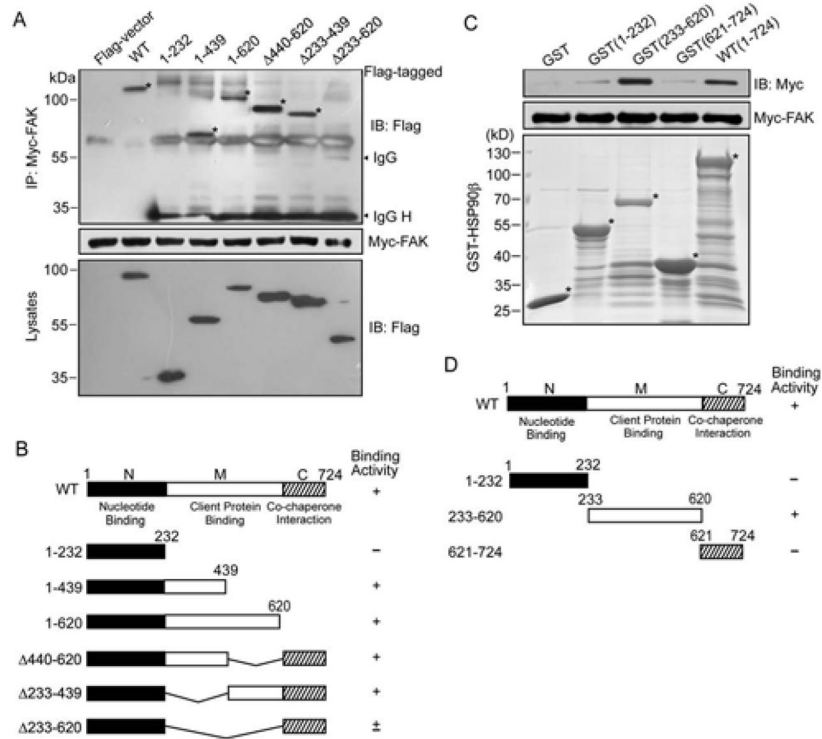


**Figure 2.**

Identification of HSP90 $\beta$  domains involved in FAK interaction. (A) Different domains of HSP90 $\beta$  interact with Myc-tagged FAK in HEK293T cells. Myc-tagged FAK, immobilized on protein-G agarose beads, was incubated with lysates from HEK293T cells expressing Flag-tagged HSP90 $\beta$  derivatives. Precipitated proteins and input lysates were immunoblotted with anti-Flag antibody. IgG H, IgG heavy chain. (B) HSP90 $\beta$  constructs and FAK binding activity. (C) Direct interaction between HSP90 $\beta$  and FAK. HEK293T cells expressing Myc-tagged FAK were lysed and resulting lysates were incubated with indicated GST-fusion proteins immobilized on Glutathione-Sepharose beads. Bound proteins were probed with anti-Myc antibodies (top). GST-fusion proteins were revealed by SDS-PAGE method and stained with Coomassie Brilliant Blue (bottom). (D) Structural domains of HSP90 $\beta$  used in these experiments and FAK binding activity. The corresponding bands are indicated with stars.

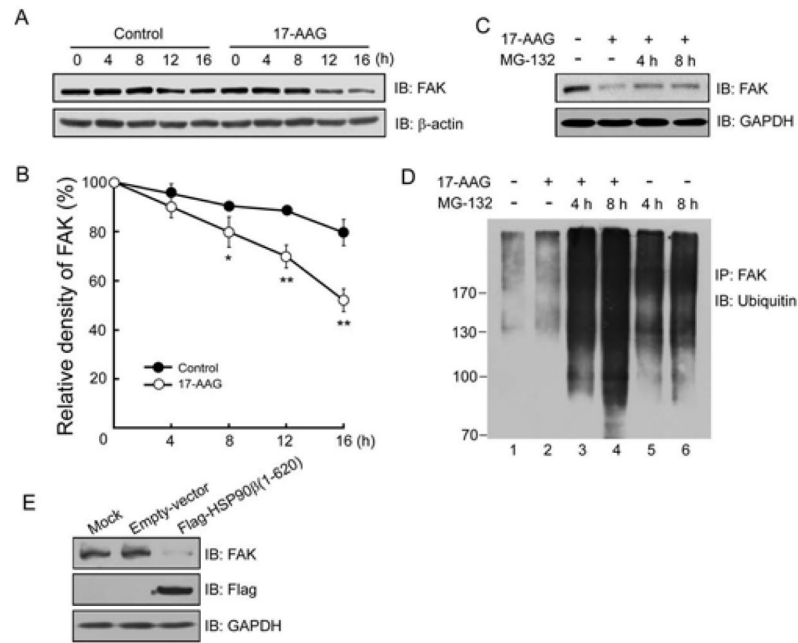


**Figure 3.**

Accelerated FAK turnover induced by 17-AAG. (A) Time-dependent reduction of FAK in 17-AAG-treated MDA-MB-231 cells. Cells were treated with CHX (50  $\mu$ g/ml) alone (control) or together with 17-AAG for the indicated times. Lysates were probed for FAK and  $\beta$ -actin (loading control). Shown were representative blots. Quantitative analysis of relative density was shown in (B) (mean  $\pm$ SD, n=3; \*  $P$  < 0.05, \*\*  $P$  < 0.01). (C) FAK reduction by 17-AAG treatment was reversed by adding MG-132. MDA-MB-231 cells were treated with vehicle (DMSO) or 17-AAG (5  $\mu$ M) for 16 h, with or without 20  $\mu$ M MG-132 for 4 h and 8 h before cell harvest. Lysates were subjected to immunoblotting with indicated antibodies. (D) FAK is ubiquitinated in response to 17-AAG treatment. MDA-MB-231 cells were treated with 5  $\mu$ M 17-AAG alone or following 4 h and 8 h preincubation with 20  $\mu$ M MG-132. Lysates were immunoprecipitated with anti-FAK and the immunoblots were probed for ubiquitin. (E) Diminished FAK levels in HSP90 $\beta$  (1–620)-expressing HEK293T cells. HEK293T cells injected with empty vector or pIRES2-Flag (1–620) were homogenized and analyzed for expression of indicated proteins.

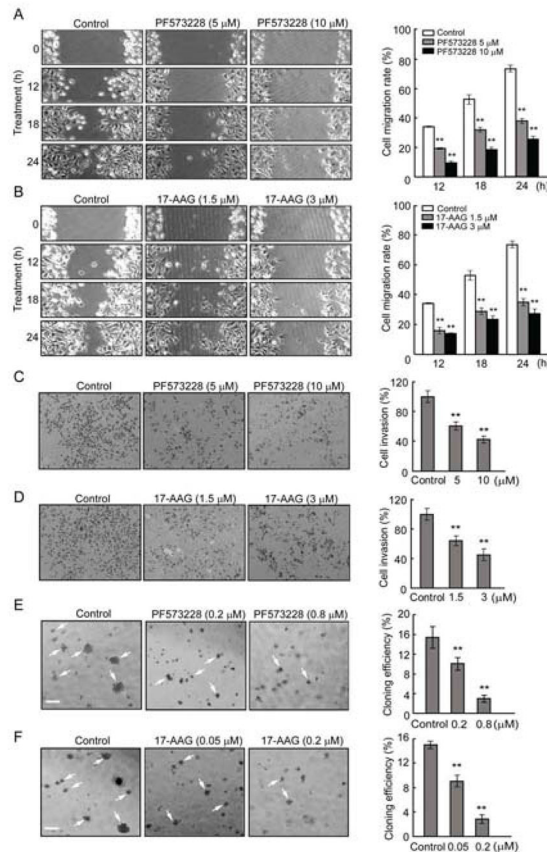


**Figure 4.**

Reduced migration, invasion and growth of MDA-MB-231 cells treated with PF573228 and 17-AAG. (A, B) Inhibition of FAK by PF573228 or inhibition of HSP90 $\beta$  by 17-AAG attenuated cell migration in a dose-dependent manner. Cell migration was quantified by measuring the difference in distance between the leading edge at the initiation of the experiment and after 12, 18, 24 h of incubation. (C, D) Decreased invasion of MDA-MB-231 cells treated by PF573228 and 17-AAG. Cell invasion was detected using a transwell assay. Representative images of inserts stained with crystal violet. Quantification of invasion cells was shown on the right. The number of invasion cells in control medium-treated wells across the inserts was set at 100%, and percentage changes over this were indicated. (E, F) Anchorage-independent growth of MDA-MB-231 cells treated with 0.2, 0.8  $\mu$ M of PF573228 or 0.05, 0.2  $\mu$ M of 17-AAG were evaluated by the colony formation efficiency (CFE). Colonies with more than 50 cells were counted by light microscopy. CFE is determined by formula as: (number of colonies formed/number of cells incubated)  $\times$  100%. Scale bar indicates 200  $\mu$ m. Error bars represent the standard deviation of three independent experiments. \*\*  $P < 0.01$ , compared with control groups.

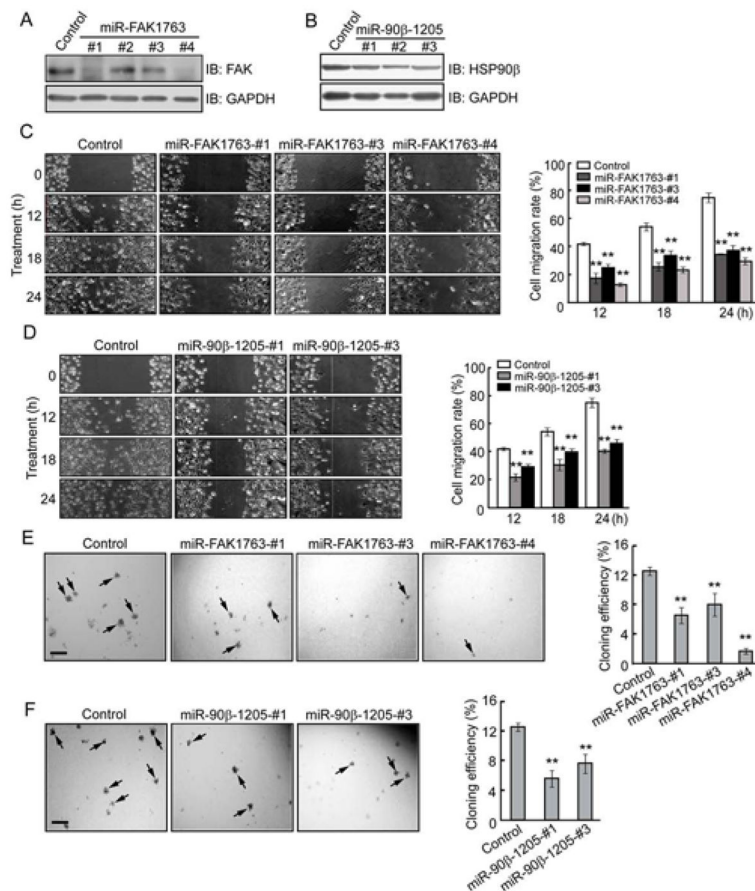


**Figure 5.**

Reduced cell migration and growth of MDA-MB-231 cells by repressing FAK or HSP90 $\beta$  expression. (A, B) Inhibition of FAK and HSP90 $\beta$  expression by miRNAi constructs. MDA-MB-231 cells were transfected with miRNAi constructs of FAK or HSP90 $\beta$ . The control miRNAi encodes scrambled sequences. Forty-eight hours after transfection, cell lysates were immunoblotted with antibodies against FAK (A), HSP90 $\beta$  (B), or GAPDH for loading control. (C, D) Migration of cells transfected with miR-FAK1763 or miR-90 $\beta$ -1205 were reduced. Cell migration was quantified by measuring the difference in distance between the leading edge at the initiation of the experiment and after 12, 18, 24 h of incubation. (E, F) Anchorage-independent growth of MDA-MB-231 cells expressed miR-FAK1763 or miR-90 $\beta$ -1205 were evaluated by the CFE as histograms. Colonies with more than 50 cells were counted by light microscopy. CFE is determined by formula as: (number of colonies formed/number of cells incubated)  $\times$  100%. Scale bar indicates 200  $\mu$ m. Error bars represent the standard deviation of three independent experiments. \*\*  $P < 0.01$ , compared with control groups.



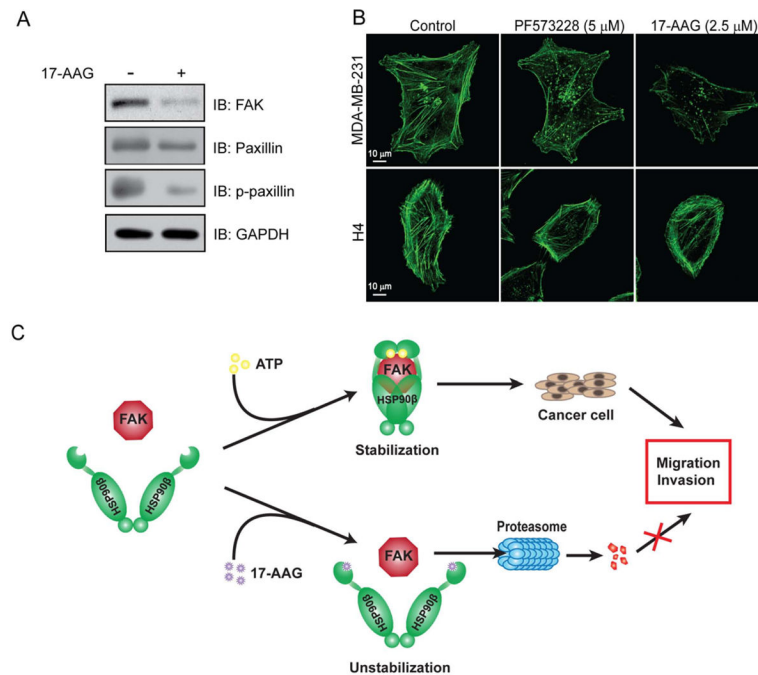


**Figure 6.** Impaired cell motility and cytoskeletal organization by treatment with FAK and HSP90 $\beta$  inhibitors. (A) HSP90 $\beta$  inhibition reduced FAK and its downstream effector-paxillin and phosphorylated paxillin (p-paxillin). (B) PF573228 and 17-AAG inhibited the organization of actin cytoskeleton in MDA-MB-231 and H4 cells. Fluorescence images of F-actin staining by Alexa Fluor 488 phalloidin of 17-AAG (2.5  $\mu$ M) or PF573228 (5  $\mu$ M) treated and untreated MDA-MB-231 and H4 cells for 15 h. Error bars represent the standard deviation of three independent experiments. \*\*  $P < 0.01$ , compared with untreated control groups. (C) A model for the role of HSP90 in FAK regulation. In MDA-MB-231 cells, HSP90 $\beta$  helps to stabilize FAK, contributing to cell migration and invasion. 17-AAG disrupts the interaction of FAK and HSP90 $\beta$ , and FAK is recognized by ubiquitin to undergo proteasome-dependent degradation, thus, attenuating tumor cell migration and invasion.